International Journal of Pharmaceutics 529 (2017) 597–607

Contents lists available at ScienceDirect

International Journal of Pharmaceutics

journal homepage: www.elsevier.com/locate/ijpharm

Discrete particle modeling and micromechanical characterization of bilayer tablet compaction

B. Yohannes[a], M. Gonzalez[b], A. Abebe[c], O. Sprockel[c], F. Nikfar[c], S. Kiang[d,1], A.M. Cuitiño[a,*]

[a] Mechanical and Aerospace Engineering, Rutgers University, Piscataway, NJ 08854, United States
[b] School of Mechanical Engineering, Purdue University, West Lafayette, IN 47907, United States
[c] Bristol-Myers Squibb Company, Drug Product Science and Technology, New Brunswick, NJ 08903, United States
[d] Chemical and Biochemical Engineering, Rutgers University, Piscataway, NJ 08854, United States

ARTICLE INFO

Article history:
Received 3 January 2017
Received in revised form 30 June 2017
Accepted 10 July 2017
Available online 13 July 2017

Keywords:
Bilayer tablets
Layer interface
Tensile strength
Discrete particle modeling
Contact area

ABSTRACT

A mechanistic particle scale model is proposed for bilayer tablet compaction. Making bilayer tablets involves the application of first layer compaction pressure on the first layer powder and a second layer compaction pressure on entire powder bed. The bonding formed between the first layer and the second layer particles is crucial for the mechanical strength of the bilayer tablet. The bonding and the contact forces between particles of the first layer and second layer are affected by the deformation and rearrangement of particles due to the compaction pressures. Our model takes into consideration the elastic and plastic deformations of the first layer particles due to the first layer compaction pressure, in addition to the mechanical and physical properties of the particles. Using this model, bilayer tablets with layers of the same material and different materials, which are commonly used pharmaceutical powders, are tested. The simulations show that the strength of the layer interface becomes weaker than the strength of the two layers as the first layer compaction pressure is increased. The reduction of strength at the layer interface is related to reduction of the first layer surface roughness. The reduced roughness decreases the available bonding area and hence reduces the mechanical strength at the interface. In addition, the simulations show that at higher first layer compaction pressure the bonding area is significantly less than the total contact area at the layer interface. At the interface itself, there is a non-monotonic relationship between the bonding area and first layer force. The bonding area at the interface first increases and then decreases as the first layer pressure is increased. These results are in agreement with findings of previous experimental studies.

© 2017 Elsevier B.V. All rights reserved.

1. Introduction

Bilayer tablets or multi-layer tablets are highly suitable for drug delivery of many therapeutic areas (Abebe et al., 2014), for controlled drug delivery of two different active ingredients (Abebe et al., 2014; Abdul and Poddar, 2004), and separation of chemically incompatible drugs (Divya et al., 2011). The production of such tablets has proved design and manufacturing challenges as the layered tablets are prone to fracture by delamination, usually along the interfaces between two layers, because of their inherent insufficient strength (Akseli et al., 2013; Kottala et al., 2012). The residual stress distribution in bilayer tablets is one of the major sources of inhomogeneity of the micromechanical properties causing the tablets to fracture and split apart (Inman et al., 2007). Thus, one of the main manufacturing challenges is to obtain tablets that do not fracture at the interface because of insufficient mechanical strength. Understanding and predicting the mechanical strength of these bilayer tablets is of commercial significance because tablet failures due to weak mechanical strength can lead to economic losses.

The mechanical strength of bilayer tablets depends on many factors. Using axial tensile strength tester, Akseli et al. (2013) experimentally studied the strength of bilayer tablets made up of microcrystalline cellulose (MCC) and starch powders. It was found that the tensile strength of the bilayer tablets increases as the second layer compaction force is increased. However, the tensile

* Corresponding author.
E-mail address: cuitino@jove.rutgers.edu (A.M. Cuitiño).
[1] Formerly at: Bristol-Myers Squibb Company, New Brunswick, NJ 08903, United States.

http://dx.doi.org/10.1016/j.ijpharm.2017.07.032
0378-5173/© 2017 Elsevier B.V. All rights reserved.

strength of the bilayer tablets does not have a monotonic relationship with the first layer compaction force. The tensile strength initially increases with the first layer compaction force and then decreases as the first layer force is increased further. It was also noted that the bilayer tablets break at the interface at large first layer compaction force (Kottala et al., 2012; Inman et al., 2009). At higher compaction force, the particles deform permanently reducing the particle asperities and irregularities. The permanent deformation, along with the rearrangement of the particles, reduces the surface roughness of the first layer. Smoother surfaces reduce the possibility of a better contact between the layers, and hence result in weaker tablets.

In addition to the applied forces, the physical and mechanical properties of the layer materials also play a critical role in the tensile strength of the tablet (Podczeck and Al-Muti, 2010; Podczeck et al., 2006; Inman et al., 2007; Busignies et al., 2013). Using a three-point bending experiment, Podczeck and Al-Muti (2010) showed that both particle size and modulus of elasticity influenced the overall strength of layered tablets/beams. They found that if the material forming the lower layer was more elastic, then the beam strength was reduced due to tension introduced into the system, acting especially at the layer interface and potentially causing partial or complete delamination. Larger differences in the particle size of the materials forming the tablet layers also resulted in an overall reduced tensile strength. In another flexure test experiment, Busignies et al. (2013) showed that the fracture occurred at the interface or in one of the two layers depending on the materials properties. In most cases, the highest tensile strength was obtained when the materials had similar elastic recovery. On the contrary, for materials with different elastic recovery, the tensile strengths were reduced.

Computational simulations can also be used to investigate detailed micromechanical properties to assess the mechanical strength of tablets. Several computational methods have been developed to model compaction of monolayer tablets, but there is no computational framework for modeling bilayer tablets. However, the methods that are used to model monolayer tablets can be modified to model bilayer or multi-layer tablets. Some of these methods are based on Finite Element Method (FEM) (Klinzing et al., 2010), Discrete Element Method (DEM) (Sheng et al., 2004; Martin and Bouvard, 2004; Skrinjar and Larsson, 2004; Olsson and Larsson, 2013; Cundall and Strack, 1979), or combined Discrete-Finite Element Method (DFEM) (Zheng and Cuitiño, 2002; Zavaliangos, 2002; Zhang, 2009; Zhang and Zavaliangos, 2011; Koynov et al., 2011). In FEM, usually, only the global values of the physical properties are assumed, while in DEM the interaction between individual particles are accounted for, which enables modeling the heterogeneity of powders at the microscopic/particle scale. Hence, DEM gives more accurate particle scale details than continuum methods that consider global physical properties of the material. DEM was originally developed for application pertaining to very small elastic deformations (Cundall and Strack, 1979). In recent years, DEM has been used to model plastic deformation (Sheng et al., 2004; Martin and Bouvard, 2004; Olsson and Larsson, 2013) and bonding between particles (Potyondy and Cundall, 2004).

Since the main difference between monolayer and bilayer tablets is the presence of a layer interface in the latter case, the computational methods developed for monolayer tablets can be used to model bilayer tablets by taking into consideration the particles at the layer interface. In this paper, we propose a contact model for particle–particle interactions at the layer interface to computationally model a bilayer tablet compaction. The model is built upon a previous model that has been shown to work for monolayer tablets (Yohannes et al., 2016). Yohannes et al. (2016) used the model to calibrate the material properties and predict the tensile strength of tablets made from MCC and lactose powders. Although, the shape of the tablet is known to influence the tensile strength of the tablet (Franck et al., 2015), this article focuses only on cylindrical flat tablets. First, the contact model for the layer interface is presented followed by comparisons of the simulation results with experimental results for bilayer tablets. Then, factors affecting the mechanical strength of the tablets are discussed based on the simulation results. Finally, challenges and possible extension of the model are presented.

2. Numerical simulation

The procedure of making a bilayer tablet computationally is similar to the procedure of making a tablet experimentally. It involves the following steps:

1. Depositing the first layer particles
2. Compacting the first layer particles (application of the first layer compaction force)
3. Removing the first layer compaction force
4. Depositing the second layer particles
5. Compacting the bilayer tablet (application of the second layer compaction force)
6. Removing the second layer compaction force, and
7. Ejecting the tablet

The steps for making monolayer and bilayer tablets are similar except for the deposition of the second layer, and application and removing of the second layer force for the bilayer tablet.

Both the first and the second layer particles were deposited using ballistic gravitational deposition method (Jullient et al., 1992; Koynov et al., 2011; Bratberg et al., 2002; Mueller, 1997; Bagi, 2005; Yohannes et al., 2016). The first layer particles were deposited on a flat surface in a cylindrical die, whereas the second layer particles were deposited on top of the first layer after the application of the first layer compaction force.

The first layer and second layer compaction forces are applied through upper and lower punches. The compaction simulation was a strain controlled simulation, where a small displacement is applied to the two punches. The pressure on the punches is computed based on the contact forces from the particles. During the compaction, unloading, and ejection simulations, the contact forces between the particles are computed based on the deformation and mechanical properties of the particles. During loading mode, the particles are restricted to follow a power-law plasticity model (Storåkers et al., 1997; Storåkers et al., 1999; Mesarovic and Johnson, 2000; Martin and Bouvard, 2004; Yohannes et al., 2016),

$$\sigma = k\varepsilon^{1/m}, \tag{1}$$

where ε and σ are strain and stress in the particles, respectively. k is the material strength parameter and m is the strain-hardening exponent. During the loading phase the contact force (F) between two particles, particle 1 and particle 2, is always compressive (compressive force is assumed positive) and is computed as

$$F = k_p a^{2+1/m}, \tag{2}$$

where k_p is a constant that is a function of of the material properties (Yohannes et al., 2016). a is the radius of the circular contact area between the pair of contacting particles. a is computed using the overlap (γ) between a pair of particles, such that

$$\gamma = (R_1 + R_2) - (\mathbf{X_1} - \mathbf{X_2})\cdot\mathbf{n_{12}}, \tag{3}$$

where **X** is the position of the particles 1 and 2. $\mathbf{n_{12}}$ is the normal unit vector along the line connecting the centers of particles 1 and 2.

The unloading process is composed of elastic unloading and adhesive traction (Mesarovic and Johnson, 2000) and the contact force F is computed as

$$F = \frac{2k_p}{\pi} a_p^{2+1/m} \left[\arcsin \left(\frac{a}{a_p}\right) - \frac{a}{a_p}\sqrt{1-\left(\frac{a}{a_p}\right)^2} \right] - \sqrt{8\pi\omega E_m} a^{3/2}, \quad (4)$$

where a_p is the radius of the contact area at the maximum F during the loading phase (Eq. (2)), ω is the bonding energy per unit area, and E_m is the effective Young's modulus. The contact between a pair of particles will be broken when the tensile force (Eq. (4)) reaches the maximum tensile force that can be sustained by the contact. The maximum tensile force that can be sustained by the contact is referred to as the bonding force b. When the bonding between a pair of particle is broken, all the elastic deformation of the particles at the contact point is recovered and only the permanent deformation (plastic deformation) of the particles remains.

In addition to the two phases (loading and unloading) described above, a new contact can be formed on the already plastically deformed surface of the particles. This type of contact particularly prevails at the interface of layers in bilayer or multilayered compacts. As mentioned earlier, the first layer particles that are on the top surface of the layer are deformed permanently due to direct contact with the upper punch. Fig. 1 shows schematics of the deformation of a particle at the surface of the first layer due to the first layer compaction force applied through a flat faced upper punch. The original particles were spherical with radius R (Fig. 1a) but were deformed as the first layer compaction force is applied (Fig. 1b). When the first layer force is removed, some of the deformation (the elastic deformation) is recovered (Fig. 1c and 2). The schematics only show the deformation at the contact area, but the schematics are not exact representations of the actual deformed shape of a particle during loading and unloading. The main purpose of the schematics is to show how the deformation and the corresponding contact force are computed at the contact surface.

During the deposition of the second layer and the application of the second layer compaction pressure (Fig. 3a and b), contacts are formed between the first layer particles and some of the second layer particles. The interaction between these first layer and second layer particles is similar to any contact between a pair of particles, except when a second layer particle touches an already plastically deformed surface of the first layer particles. In such cases, Eq. (3) is modified to compute the overlap at the interface

$$\gamma_{int} = (R_1 + R_2 - \gamma_p) - (\mathbf{X_1} - \mathbf{X_2})\cdot\mathbf{n_{12}}, \quad (5)$$

where γ_p is the permanent deformation of the first layer particle due to the first layer compaction pressure. The radius of contact between the second layer particles and the plastically deformed surface of first layer particles (a_{int}) is computed based on γ_{int}. Accordingly, the contact force, F, during the loading and unloading phases are computed by substituting a by a_{int} in Eqs. (2) and (4).

As shown in Fig. 2a, no contact force will develop when the particles are not in contact ($\gamma_{int} < 0$). When $\gamma_{int} > 0$, there will be a contact force between the particles. If $\gamma_{int} < \gamma_p$ (Fig. 2b), we assume that the bonding between the particles is negligible and the contact force can only be compressive. If the unloading process starts before $\gamma_{int} >= \gamma_p$, only the first term in Eq. (4) is used to compute the contact force. Bonding between a pair of contacting particles is formed only when $\gamma_{int} > \gamma_p$ (Fig. 2c). These assumptions about the interaction of particles at the interface are the key factors that distinguish bilayer or multilayered tablets from a monolayer tablet.

3. Experimental validation

To validate our model, the simulations results are compared to bilayer tablet compaction experiments. In the simulations, mechanical properties of particles as reported in Yohannes et al. (2016) are used. Yohannes et al. (2016) have shown a method to calibrate the mechanical properties of the particles and validate powder compaction simulations based on experimental tablet compaction and tensile strength tests. The calibration of the mechanical properties was done by comparing the compressibility, compaction pressure vs. relative density curve, of the powders. Since the plastic parameters k and m have a significant role during the compaction of the powder bed, these parameters were calibrated using the compaction pressure vs. relative density curve during the application of the compaction pressure. The calibration involved running several compactions simulations with several combinations of the plastic parameters k and m. The least mean square approach was used to identify the best fitting combination of k and m. Once the plastic parameters, k and m, were selected, the effective Young's modulus (E_m) and the bonding energy (ω) were calibrated using the unloading phase in the compaction vs. relative density curve. As in the calibration of the plastic parameters, several combinations of E_m and ω were tested and the least mean square approach was used to identify the best fitting combination of E_m and ω. The calibrated mechanical

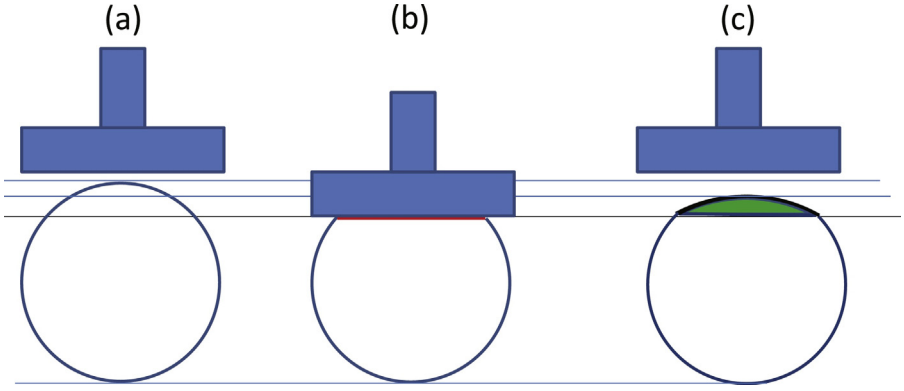

Fig. 1. Schematics of deformation particles (a) before, (b) during, and (c) after application of first layer compaction pressure. The schematics only show the deformation at the contact area, which is not exact representation of the actual deformed shape of a particle during loading and unloading. The main purpose of the schematics is to show how we calculate the deformation and the corresponding contact force at the contact surface.

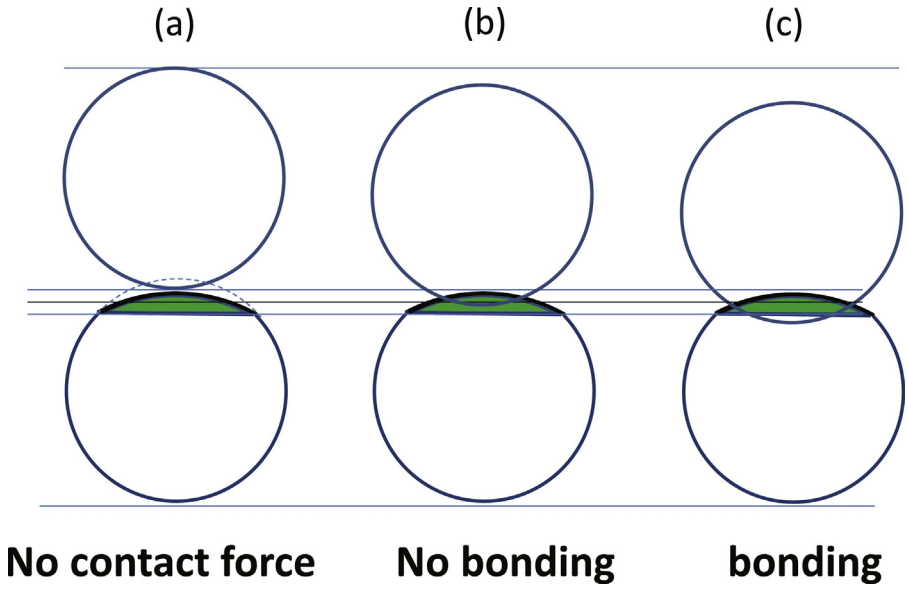

Fig. 2. Schematics of contact forces between deformed first layer particles (bottom row) and virgin second layer particles (top row): (a) no contact between the particles, (b) there is compression contact force but no bonding is formed between the particles, and (c) bonding is formed between the particles.

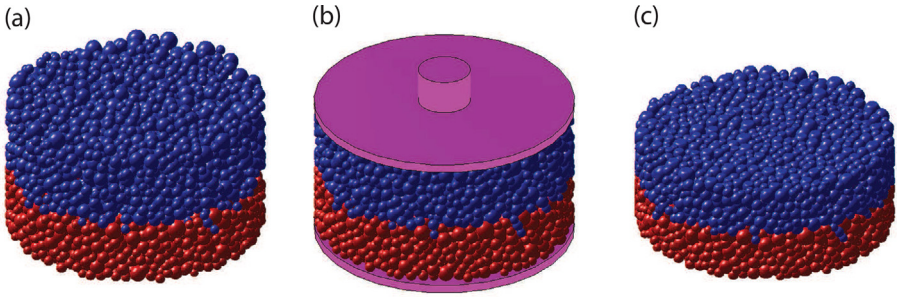

Fig. 3. Compaction of lactose–lactose bilayer tablet: first layer particles (red) and second layer particles (blue); (a) deposition of second layer particles on already compacted first layer particles, (b)application of second layer force, and (c) bilayer tablet after tablet is ejected. (For interpretation of the references to color in this figure legend, the reader is referred to the web version of the article.)

properties were validated by comparing the tensile strength test results of the simulations with that of the experiments. Since materials that were used in Yohannes et al. (2016) are also used in the current study, there was no need to calibrate the mechanical properties of the materials for the simulations. Table 1 shows the material properties of two commonly used pharmaceutical powders, lactose monohydrate (Foremost Farms, Baraboo, WI) and microcrystalline cellulose (MCC-Avicel PH102, FMC Biopolymer, Newark, DE) as reported by Yohannes et al. (2016).

In the experiments, the true density (ρ_{true}) of MCC and lactose was measured using a AccuPyc Pycnometer (AccuPyc II 1340 V1.05 Unit 1 Serial No. 622) and helium as analysis gas (Yohannes et al., 2015). The samples were dried at 50 °C overnight before the density test. In addition, than 100 μm were used in both the experiments and the simulations. Yohannes et al. (2015) have shown that removing the fine particles does not affect the compaction and tensile strength of the tablets. Using particle sizes greater than 100 μm improves the computational efficiency in the simulations as it significantly reduces the total number of particles in the tablet. The sizes of particles used in this study range between 100 and 240 μm for lactose and between 100 and 750 μm for MCC (Fig. 4). The particle size distribution of the powders are exactly represented in the deposition and compaction simulations.

Though no particle fragmentation was considered and only spherical particles were used by Yohannes et al. (2016) and in the current research, the compressibility profile and the tensile strength of the tablets in the simulations compares well with the experimental results of lactose and MCC powders, which were composed of irregular particles (Yohannes et al., 2015). Johansson and Alderborn (2001) have shown that the irregular shape of particles causes complex compression behavior, attrition of the particles, and increased bed void. This indicates that the mechanical properties used in the simulations indirectly account for irreversible process such as particle fragmentation.

The bilayer tablet compaction experiments were done using a Presster machine (The Metropolitan Computing Corporation of East Hanover, NJ). The powders are compacted using a 10 mm flat round face tooling. At the start of the experiments, the die wall was lubricated with MgSt using a cotton swab. A Kikusui Libra-2 tablet press was emulated at 16.4 rpm, which is the lowest compaction speed for this press type. A low compaction speed is used to ensure that the compaction process is independent of the rate of material

Table 1
Material and physical properties from experiments and simulations by Yohannes et al. (2015) and Yohannes et al. (2016), respectively.

Powder	k (MPa)	m	E (MPa)	ω (J/m^2)	ρ_{true} (g/cc)
Lactose	375	1.0	10	1100	1.53
MCC	150	4.0	5	400	1.54

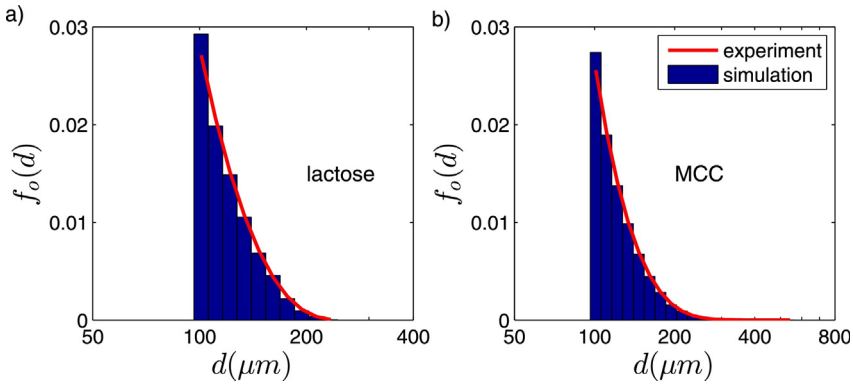

Fig. 4. Particle size distribution for (a) lactose and (b) MCC powders used in the experiments and simulations. The distribution function, f_o(d) is based on the number of particles. Note that the horizontal axis in logarithmic scale and the area under the curve is one (Yohannes et al., 2016).

deformation. It has been known that the tableting speed can affect the tabletability and compressibility of some materials such as MCC, starch, lactose, and dicalcium phosphate (Tye et al., 2005). Compaction forces are measured using strain gauges placed on the compression roll pins. Since the forces on the upper and lower punches were almost the same, only the force on the upper punch is used for computing the compaction pressure. No precompression force was applied for these experiments. Punch displacement is measured using a linear variable displacement transducer (LVDT; 250MHR, Schaevitz, USA) connected to each punch.

In order to control the mass of each layer accurately, the powder for each layer was poured in the die manually. The two layers have equal amount of material: 150 mg each. Initially, 150 mg of powder is measured separately on a scale and poured in the die. Then, a compaction force (i.e. first layer force) is applied on the powder. Another batch of 150 mg of powder is poured in the die manually on top of the already compacted first layer powder. Then, a compaction force (i.e. second layer force) is applied on the two layers. The density (ρ) of the powder during compaction is computed as the ratio of the total mass of the powder in the die and the total volume (V_T) of the powder in the die ($\rho = mass/V_T$). The total volume is computed as $V_T = \pi d^2 h/4$, where $d = 10$ mm is the diameter of the die and h is the thickness of the powder bed which is measured using the displacement transducer connected to each

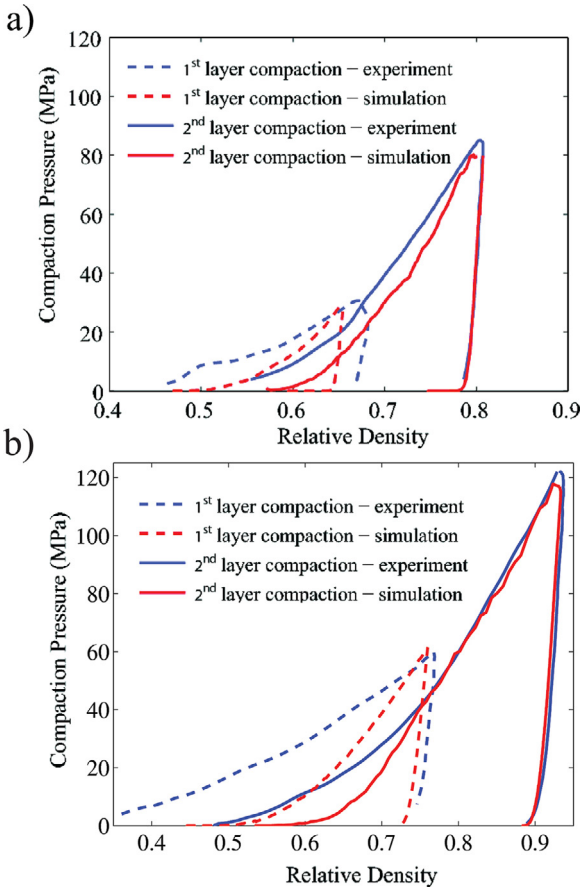

Fig. 5. Comparison of experimental and numerical compaction profile for bilayer tablet compaction: (a) Lactose–lactose bilayer tablet and (b) MCC–MCC bilayer tablet.

punch. The relative density can then be computed as the ratio of the density and true density (relative density = ρ/ρ_{true}). Therefore, the thickness of the first layer during the application of first layer force is known. However, during the application of the second layer force, it was not possible to measure the thickness of the layers separately.

4. Results and discussion

In the experiments, the initial relative densities for lactose and MCC powders were 0.47 and 0.35, respectively (Yohannes et al., 2015). These values are lower than the theoretical possible relative densities for a packing of spherical particles. The lower initial densities are due to the irregular shape of the particles (Zou and Yu, 1996; Yohannes et al., 2015) and inter-particle attractive forces (Castellanos, 2005). In the simulations, however, only spherical particles are used and the inter-particle attractive force is ignored. The initial relative density after the ballistic deposition simulations for both lactose and MCC was about 0.5, which was the main difference between the experiments and the simulations.

Fig. 5 shows comparison of experimental and computational compaction profiles for bilayer tablets. Fig. 5a shows a bilayer tablet where the first and second layers material is lactose (referred in this article as lactose–lactose bilayer tablet). The compaction profiles for both the first layer and second layer compaction pressures from the simulations are compared to that of the experiment. The first layer compaction pressure was about 30 MPa and the second layer compaction pressure was about 80 MPa. After the first layer compaction force is removed, the relative density of the compacted first layer was about 0.65. When the second layer powder is filled(deposited) in the die, the relative density of the powder bed decreases to about 0.55. The main reason for the reduction of the relative density is the low *initial* relative density of the second layer powder. Fig. 5b shows simulation and experimental result for MCC–MCC bilayer tablet. The first layer compaction pressure was about 30 MPa and the second layer compaction pressure was about 120 MPa. The results from the simulation are quantitatively close to those of the experiment with some differences. The main differences are, as mentioned earlier, the initial relative density of the powder bed during deposition and the compressibility during early stages of compaction (Yohannes et al., 2015). However, the values of the compaction forces in the simulations and experiments were similar at the peak first layer compaction pressure. In addition, the compressibility profile during the application and unloading of the second layer in the simulations compares well with that of the experiments. Considering that the material properties were calibrated only for a monolayer tablet and the simplicity of the proposed contact law at the interface, the differences in the simulations and experimental results are not significant. Therefore, these simulations are used to study the effect of the first and second layer materials and compaction pressures on the mechanical strength of bilayer tablets.

As the first layer force is applied, the particles rearrange and deform, and hence the inter-particle compression force, and inter-particle bonding increase (Yohannes et al., 2016). When the first layer compaction pressure is removed, the compact relaxes. The relaxation of the tablet can reach up to 10% depending on the compaction pressure (Yohannes et al., 2015). Due to this relaxation, the inter-particle compression force decreases, but the permanent deformation (the plastic deformation) of the particles remains. For bilayer tablet application, the permanent deformation of the particles at the top surface of the first layer is of a particular interest. The permanent deformation and the arrangement of the surface particles directly affect the roughness of the surface.

The surface roughness of the first layer in the simulations is computed by partitioning the surface of the first layer into small rectangular cells (5 μm × 5 μm) and measuring the elevation (y) of each cell. The elevation of the center of each cell is computed based on the size, deformation, and position of the particles. Then, the

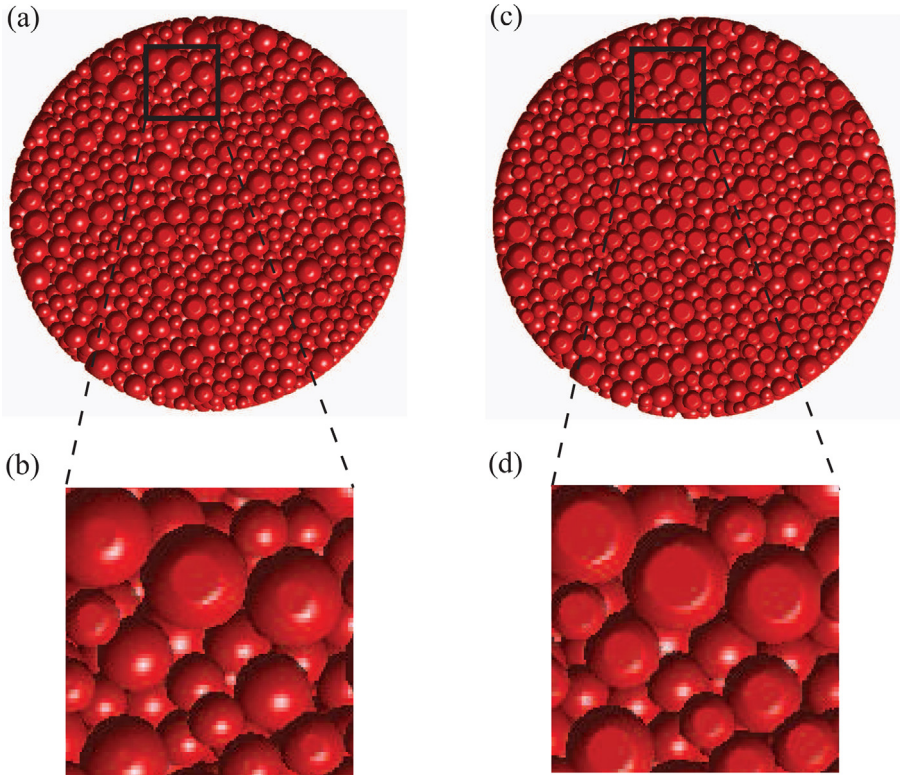

Fig. 6. Deformation of first layer lactose particles due to first layer compaction pressure of 30 MPa (a and b) and 95 MPa (c and d).

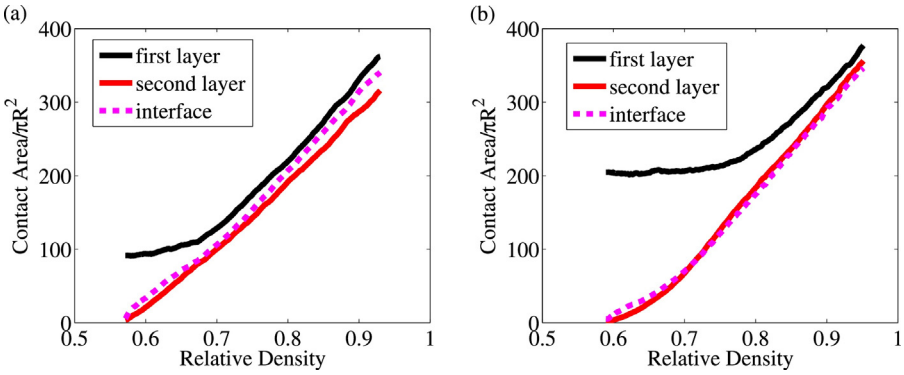

Fig. 7. Total contact area vs. relative density for lactose–lactose bilayer tablet in the layers and at the interface during application of second layer force. The first layer compaction pressure was (a) 30 MPa and (b) 95 MPa. The contact area is normalized by the cross-sectional area of the smallest particle.

roughness is computed as the ratio of the standard deviation (σ) and the largest radius of the particles: roughness $= \frac{\sigma}{R_{\max}}$, where R_{max} is the maximum radius of the particles. $\sigma = \sqrt{\frac{\sum_{i=1}^{n}(y_i - \bar{y})^2}{n}}$, where $\bar{y}$ is the average elevation and n is the number of cells. σ was normalized by R_{max} for easier comparison of the particle size and the surface roughness. $R_{max} = 118\ \mu m$ and $R_{max} = 360\ \mu m$ for lactose and MCC powders, respectively. Fig. 6 shows the image of the first layer (lactose) surface for first layer compaction pressures of 30 MPa and 95 MPa. At larger compaction pressure, the particle deform more and result in a reduced surface roughness. The roughness was 0.4 and 0.3 for the 30 MPa and 95 MPa first layer pressures, respectively.

Prior studies have shown that high first layer roughness provides more surface area for bonding between first layer and second layer particles (Akseli et al., 2013; Kottala et al., 2012). These studies indicated that the bonding area is directly associated with the tensile strength of the tablet. Therefore, measuring the bonding area provides information about the tensile strength of the bilayer tablets, particularly, when the same material is used in both layers. As described in the previous section, the contact law at the interface is slightly different from that of the layers due to the deformation of the first layer surface particles by the first layer compaction pressure. For example, if there is no application of first layer compaction pressure (no deformation of first layer particles), a bilayer tablet with identical powders in the layers should be similar to a monolayer tablet. The cumulative bonding/contact area is uniform across any given horizontal plane in the tablet and increases as the compaction pressure is increased (Yohannes et al., 2016). Moreover, there is no difference between the contact area and the bonding area (the contact area when there is bonding between particles).

If a first layer compaction force is applied, there can be a difference between the contact area and the bonding area. Fig. 7 shows the evolution of total contact area during the application of the second layer pressures for two cases, where the first layer compaction pressures was 30 MPa and 95 MPa. The bonding/contact area in the layers is computed across a given horizontal plane in each layer, whereas the bonding/contact area at the interface is computed as summation of contact areas between first layer and second layer particles. Initially, the contact area in the first layer is larger than those in the second layer and at the interface. This is because contact area has already been formed in the first layer material during the first layer compaction. Also, the initial first layer contact area is larger for the tablet with higher first layer compaction pressure. At the early stages of the application of the second layer pressure, the contact area in the first layer remains constant, until the relative density reaches about 0.65 and 0.75 for the first layer pressures of 30 MPa and 95 MPa, respectively. These relative densities are very close to the relative density of the first layer after the application of the first layer force. This indicates that the contact area in the first layer does not change until the value of the relative density of the bilayer tablet reaches the relative density of the first layer powder after the application the first layer pressure. Unlike the first layer, the contact area in the second layer and at the interface grow continuously as the second layer pressure is applied. From these relative densities onwards, the contact areas in both layers and at

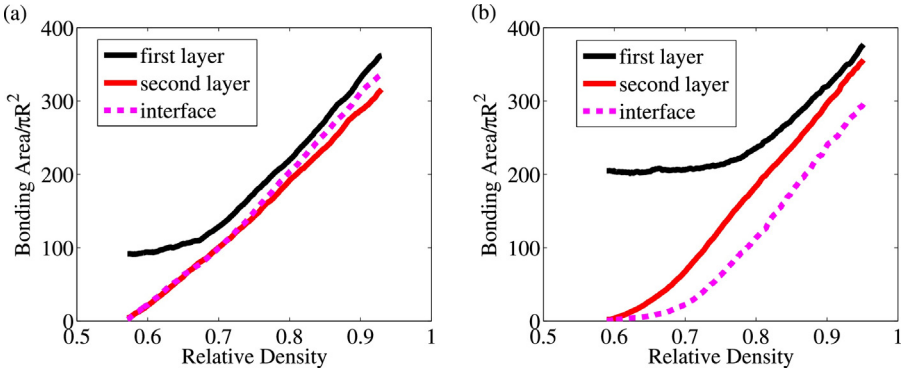

Fig. 8. Bonding area vs. relative density for lactose–lactose bilayer tablet in the layers and at the interface during application of second layer force. The first layer compaction pressure was (a) 30 MPa and (b) 95 MPa. The bonding area is normalized by the cross-sectional area of the smallest particle.

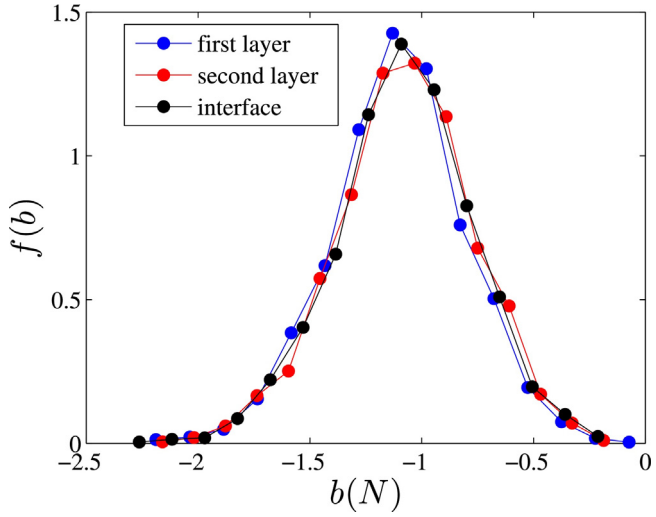

Fig. 9. Probability distribution of the tensile force that can be supported by the particle–particle contact in the layer and at the interface for first layer pressure of 95 MPa and second layer pressure of 210 MPa for lactose–lactose bilayer tablet.

the interface grow at the same rate. Therefore, the compaction pressure and the relative density are directly related to the total contact area. However, as mentioned earlier, the total contact area alone cannot be used to estimate the tensile strength of the tablet.

Tensile strength is generated due to the bonding between particles, which can be related to the bonding area between particles. Fig. 8a and b shows the bonding area in the layers and at the interface for first layer compaction pressures of 30 MPa and 95 MPa, respectively. For the 30 MPa case, the total contact area (Fig. 7) is very similar to the bonding area. Therefore, at low first layer compaction pressure, the deformation of the particles and the reduction in the surface roughness of the first layer did not cause a significant change in the bonding area at the interface. Further, at this low pressure, the bonding areas in the layers and at the interface are very similar, which indicates that the layers and the interface have similar the tensile strength. However, at higher first layer compaction pressure, the bonding area is significantly smaller than the total contact area at the layer interface. Particularly, no bonding area is formed at the interface during the early phase of application of second layer compaction pressure. Since the interface has a lower bonding area than those in the layers, the bilayer tablet will break at the interface when an axial tensile force is applied.

In addition, the maximum tensile force that can be supported at every inter-particle contact (referred here as the bonding force b) can be computed using Eq. (4). Fig. 9 shows the probability distribution function of b for a lactose-lactose bilayer tablet, where first layer and second layer compaction pressures were 95 MPa and 210 MPa, respectively. The distribution of b is computed after the tablet is ejected from the die. The values of b for the first and second layer are computed across a horizontal plane approximately at mid sections of the two layers. At the interface, b is computed for all contacts between the first layer and second layer particles. The distributions of b for both layers and for the interface are very similar, showing that the characteristics, such as range and magnitude of the bonding forces, are similar. However, the similarity in the pdf's does not represent similarity in the total tensile force that can be supported (referred here as the total bonding force B) across the horizontal plane in the layers and at every contact at the interface. B is computed as the sum of all values of b. Fig. 10 shows the axial component of B for the same tablet used in Fig. 9 during the application of the second layer compaction pressure. The value of B is significantly lower at the

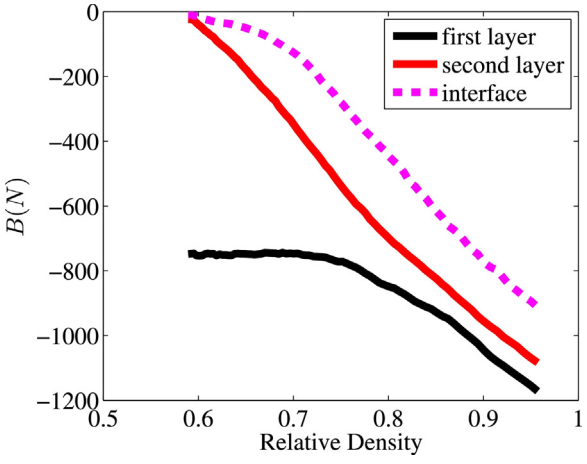

Fig. 10. The summation of the tensile force that can be supported by particle–particle contact in the layers and at the interface for first layer compaction pressure of 95 MPa for lactose–lactose bilayer tablet.

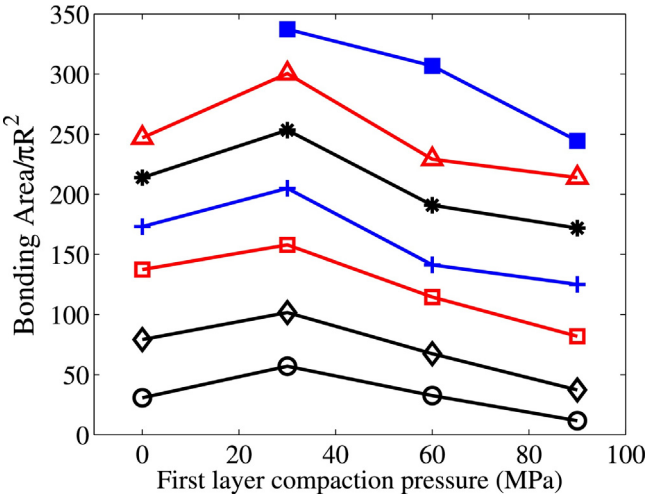

Fig. 11. Bonding area at the interface for lactose–lactose bilayer tablet at second layer compaction pressures of 30 MPa (○), 60 MPa (◇), 90 MPa(□), 120 MPa (+), 150 MPa (*), 180 MPa (△), 210 MPa (■).

interface compared to that of the layers. The value of B follows a similar trend as that of the bonding area shown in Fig 8 . Based on these, it can be concluded that the total bonding force is directly related to the bonding area. Therefore, a qualitative analysis of the mechanical strength of the tablet can be done using either the total bonding force or the bonding area.

Fig. 11 shows the bonding area at the interface for different first layer and second layer compaction pressures after the tablet is ejected from the die. The first layer pressure ranged between 0 MPa and 95 MPa, while the second layer pressure ranged between 30 MPa and 210 MPa. The bonding area increases monotonically with the second layer compaction pressure as indicated by different symbols in Fig. 11. However, the bonding area does not have a monotonic relationship with the first layer pressure. The bonding area reaches the peak at first layer pressure of 30 MPa, but decreases as the first layer pressure is increased further. These results are consistent with the findings of previous experimental studies on the strength of bilayer tablets (Akseli et al., 2013; Kottala et al., 2012). The experiments by Akseli et al. (2013) have shown that the axial tensile strength of MCC–MCC and MCC–starch bilayer tablets follows similar trends as shown in Fig. 11.

So far, our discussion on the simulations was limited to bilayer tablets where the first and second layer materials are the same (lactose–lactose and MCC–MCC bilayer tablets). The results for MCC–MCC bilayer tablets are qualitatively similar to lactose–lactose bilayer tablets. However, in some cases the materials in the first and second layers can be different. The computational modeling procedure for layers of different materials is exactly the same as layers of the same material. The mechanical properties of each layer should be first estimated using monolayer tablet compaction. Then, the effective plastic and elastic parameters for interaction between different materials at the layer interface can be computed using Eqs. (2)–(4). However, the bonding energy (ω) between two different materials can only be predicted from direct experiments. If the value of ω between two particles of different materials is available, the proposed model can be used to model a bilayer tablet with different layer materials.

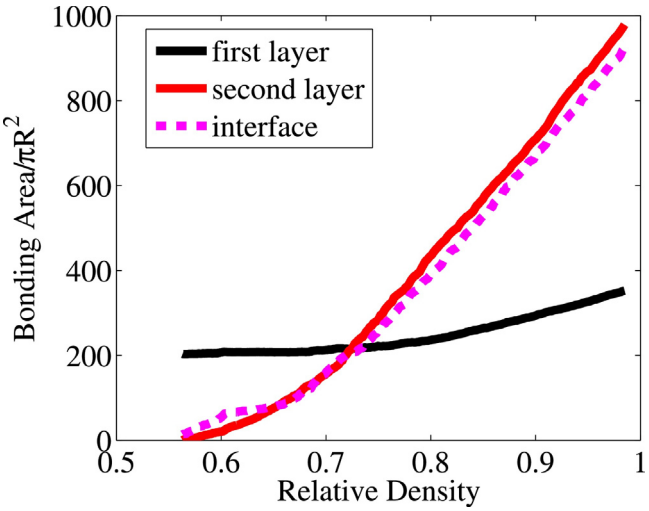

Fig. 12. Bonding area vs. relative density in both layers and at the interface during application of second layer pressure for lactose–MCC bilayer tablet. The bonding area is normalized by the cross-sectional area of the smallest particle.

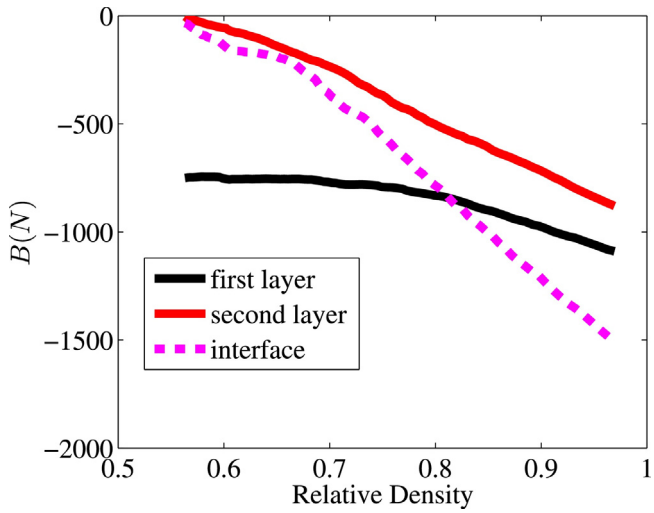

Fig. 13. The summation of the tensile force that can be supported by particle–particle contact in the layers and at the interface for lactose–MCC bilayer tablet.

In situations where the first and second layer materials are different, the bonding area is not the only factor that determines the relative strength of the layers and the interface. The mechanical properties of each material also need to be considered. As a demonstration, a bilayer tablet made of lactose (first layer) and MCC (second layer) (lactose–MCC bilayer tablet) is tested. At the interface, ω is assumed to be a harmonic mean of the bonding energy of the first and second layer particles

$$\omega_{int} = \frac{2(\omega_1 \times \omega_2)}{\omega_1 + \omega_2}, \tag{6}$$

where ω_{int} is the bonding energy between the first and second layer particles. Fig. 12 shows the bonding area for lactose-MCC bilayer tablet for first layer pressure of 95 MPa. At the end of compaction, the contact area between the lactose particles (first layer) is much smaller than those of the MCC particles (second layer) and at the layer interface. However, it should be noted that lactose particles have larger plastic, elastic, and bonding parameters than that of MCC. Therefore, smaller bonding area can support larger tensile force in the case of lactose particles. Fig. 13 shows the total bonding force in the axial direction. As the second layer force is increased, the bonding force increases in the layers as well as at the interface. Though, the contact area is smaller for the first layer (lactose), the total bonding force is greater for this layer than that of the second layer. At higher second layer forces, the total bonding force is larger at the interface, which is not usually the case for bilayer tablets. The main reason for the unusual high bonding force at the interface is most likely due to error in the estimated bonding energy between MCC and lactose particles at the interface.

5. Conclusion

A contact model for the particle–particle interactions at the interface of a bilayer tablet is proposed. The model takes into consideration the elastic and plastic deformations of the first layer particles due to the first layer compaction pressure, in addition to the mechanical and physical properties of the particles. The elastic and plastic particle deformations affect the contact force and the bonding between particles of the first layer and second layer. In this model, no bonding between the interface particles will be formed until the deformation exceeds the total deformation of the first layer particle caused by the first layer compaction.

A discrete particle method based on the proposed model is used to study compaction of bilayer tablets and predict the behavior of the axial tensile strength of the tablets. Lactose and MCC, which are two of the most commonly used pharmaceutical powders, are used in the simulations. The material properties of the powders were calibrated using experiments of monolayer tablets. These material properties are used, without any change, in the bilayer tablet simulations. The simulation results are in agreement with findings of prior experimental results. As the first layer force is increased, the layer interface becomes weaker than the layers. The main reason for this is the reduced first layer surface roughness due to large first layer compaction pressure. The reduced roughness causes a decrease in the available bonding area and hence reduces the strength of the interface. In addition, the fact that there is no bonding between particles of the first and second layer particles until the deformation exceeds the permanent deformation of the first layer particles contributes to the reduced strength at the interface. In general, the bonding area is found to be significantly less than the total contact area at the interface. Further, at the interface itself, there is a non-monotonic relationship between bonding area and first layer compaction pressure. The bonding area first increases but then decreases as the first layer compaction pressure is increased.

This model can also be used for bilayer tablets where the first and second layer materials are different. The only parameter that must be determined directly from experiments is the bonding energy between the two species. This model can also be easily extended to multilayered powder compacts by repeating the model for the deformation of the first layer particles for all layers.

Acknowledgements

We gratefully acknowledge the funding for this research provided by Bristol-Myers Squibb Company. We also acknowledge the support provided by the National Science Foundation Engineering Research Center for Structured Organic Particle Systems (C-SOPS).

References

Abdul, S., Poddar, S., 2004. A flexible technology for modified release of drugs: multi layered tablets. J. Control. Release 97 (3), 393–405.
Abebe, A., Akseli, I., Sprockel, O., Kottala, N., Cuitiño, A.M., 2014. Review of bilayer tablet technology. Int. J. Pharm. 461, 549–558.

Akseli, I., Abebe, A., Sprockel, O., Cuitiño, A.M., 2013. Mechanistic characterization of bilayer tablet formulations. Powder Technol. 236, 30–36.
Bagi, K., 2005. An algorithm to generate random dense arrangements for discrete element simulations of granular assemblies. Granul. Matter 7 (1), 31–43.
Bratberg, I., Radjai, F., Hansen, A., 2002. Dynamic rearrangements and packing regimes in randomly deposited two-dimensional granular beds. Phys. Rev. E 66, 031303.
Busignies, V., Mazel, V., Diarra, H., Tchoreloff, P., 2013. Role of the elasticity of pharmaceutical materials on the interfacial mechanical strength of bilayer tablets. Int. J. Pharm. 457 (1), 260–267.
Castellanos, A., 2005. The relationship between attractive interparticle forces and bulk behaviour in dry and uncharged fine powders. Adv. Phys. 54 (4), 263–376.
Cundall, P.A., Strack, O.D.L., 1979. A discrete numerical model for granular assemblies. Geotechnique 29, 47–65.
Divya, A., Kavitha, K., Kumar, M.R., Dakshayani, S., Singh, S.D.J., 2011. Bilayer tablet technology: an overview. J. Appl. Pharm. Sci. 1, 43–47.
Franck, J., Abebe, A., Keluskar, R., Martin, K., Majumdar, A., Kottala, N., Stamato, H., 2015. Axial strength test for round flat faced versus capsule shaped bilayer tablets. Pharm. Dev. Technol. 20, 139–145.
Inman, S., Briscoe, B., Pitt, K., 2007. Topographic characterization of cellulose bilayered tablets interfaces. Chem. Eng. Res. Des. 85 (7), 1005–1012.
Inman, S., Briscoe, B., Pitt, K., Shiu, C., 2009. The non-uniformity of microcrystalline cellulose bilayer tablets. Powder Technol. 188 (3), 283–294.
Johansson, B., Alderborn, G., 2001. The effect of shape and porosity on the compression behaviour and tablet forming ability of granular materials formed from microcrystalline cellulose. Eur. J. Pharm. Biopharm. 52 (3), 347–357.
Jullient, R., Pavlovitch, A., Meakin, P., 1992. Random packings of spheres built with sequential models. J. Phys. A Math. Gen. 25, 4103–4113.
Klinzing, G.R., Zavaliangos, A., Cunningham, J., Mascaro, T., Winstead, D., 2010. Temperature and density evolution during compaction of a capsule shaped tablet. Comput. Chem. Eng. 34 (7), 1082–1091.
Kottala, N., Abebe, A., Sprockel, O., Akseli, I., Nikfar, F., Cuiti no, A.M., 2012. Influence of compaction properties and interfacial topography on the performance of bilayer tablets. Int. J. Pharm. 436, 171–178.
Koynov, A., Akseli, I., Cuiti no, A., 2011. Modeling and simulation of compact strength due to particle bonding using hybrid discrete-continuum approach. Int. J. Pharm. 418, 273–285.
Martin, C., Bouvard, D., 2004. Isostatic compaction of bimodal powder mixtures and composites. Int. J. Mech. Sci. 46 (6), 907–927.
Mesarovic, S.D., Johnson, K., 2000. Adhesive contact of elastic-plastic spheres. J. Mech. Phys. Solids 48 (10), 2009–2033.
Mueller, G.E., 1997. Numerical simulation of packed beds with monosized spheres in cylindrical containers. Powder Technol. 92 (2), 179–183.
Olsson, E., Larsson, P.-L., 2013. A numerical analysis of cold powder compaction based on micromechanical experiments. Powder Technol. 243, 71–78.
Podczeck, F., Al-Muti, E., 2010. The tensile strength of bilayered tablets made from different grades of microcrystalline cellulose. Eur. J. Pharm. Sci. 41, 483–488.
Podczeck, F., Drake, K., Newton, J., Haririan, I., 2006. The strength of bilayered tablets. Eur. J. Pharm. Sci. 29, 361–366.
Potyondy, D.O., Cundall, P.A., 2004. A bonded-particle model for rock. Int. J. Rock Mech. Min. Sci. 41 (8), 1329–1364.
Sheng, Y., Lawrence, C., Briscoe, B., Thornton, C., 2004. Numerical studies of uniaxial powder compaction process by 3d dem. Eng. Comput. 21 (2/3/4), 304–317.
Skrinjar, O., Larsson, P.-L., 2004. Cold compaction of composite powders with size ratio. Acta Mater. 52 (7), 1871–1884.
Storåkers, B., Biwa, S., Larsson, P.-L., 1997. Similarity analysis of inelastic contact. Int. J. Solids Struct. 34 (24), 3061–3083.
Storåkers, B., Fleck, N., McMeeking, R., 1999. The viscoplastic compaction of composite powders. J. Mech. Phys. Solids 47 (4), 785–815.
Tye, C.K., Sun, C.C., Amidon, G.E., 2005. Evaluation of the effects of tableting speed on the relationships between compaction pressure, tablet tensile strength, and tablet solid fraction. J. Pharm. Sci. 94 (3), 465–472.
Yohannes, B., Gonzalez, M., Abebe, A., Sprockel, O., Nikfar, F., Kiang, S., Cuitiño, A., 2016. Evolution of the microstructure during the process of consolidation and bonding in soft granular solids. Int. J. Pharm. 503, 68–77.
Yohannes, B., Gonzalez, M., Abebe, A., Sprockel, O., Nikfar, F., Kiang, S., Cuitiño, A., 2015. The role of fine particles on compaction and tensile strength of pharmaceutical powders. Powder Technol. 274, 372–378.
Zavaliangos, A., 2002. A multiparticle simulation of powder compaction using finite element discretization of individual particles. MRS Proc. 731.
Zhang, J., 2009. A study of compaction of composite particles by multi-particle finite element method. Compos. Sci. Technol. 69 (13), 2048–2053.
Zhang, J., Zavaliangos, A., 2011. Discrete finite-element simulation of thermoelectric phenomena in spark plasma sintering. J. Electron. Mater. 40 (5), 873–878.
Zheng, S., Cuitiño, A.M., 2002. Consolidation behavior of inhomogeneous granular beds of ductile particles using a mixed discrete-continuum approach. KONA Powder Particle J. 20, 168–177.
Zou, R.P., Yu, A.B., 1996. Wall effect on the packing of cylindrical particles. Chem. Eng. Sci. 51 (7), 1177–1180.